Stress-enhanced dissolution and delamination wear of crystal CaF$_2$ in water condition

Jian Gong[a,b], Chen Xiao[a], Jiaxin Yu[c], Jinfang Peng[a], Bingjun Yu[a], Lei Chen[a,b,*], Linmao Qian[a]

[a] Tribology Research Institute, State Key Laboratory of Traction Power, Southwest Jiaotong University, Chengdu 610031, China
[b] National United Engineering Laboratory for Advanced Bearing Tribology, Henan University of Science and Technology, Luoyang 471023, China
[c] Key Laboratory of Testing Technology for Manufacturing Process, Ministry of Education, Southwest University of Science and Technology, Mianyang 621010, China

ABSTRACT

The role of water in the material removal of single crystal calcium fluoride (CaF$_2$) was studied using a scratch tester with a diamond tip. Water can facilitate the sliding wear of CaF$_2$, and the degree strongly depended on the amount of water molecules involved in the wear process. CaF$_2$ wear increases with the increase of relative humidity (RH). When the sliding wear tests were conducted in dry condition, the wear rate increases linearly with applied load, obeying the Archard wear equation. When water participated in the wear process, the Archard wear equation was failure and a exponential dependence of wear rate on contact stress was given under water condition. The transformation of the applied load (or contact stress) dependence indicates the change of wear mechanism in water condition. In dry condition, the surface damage of CaF$_2$ is mainly attributed to mechanical wear where the stress-induced plastic flow under the activation of the slip systems results in a relatively smooth worn surface. In humid nitrogen or water condition, the plastic wear of CaF$_2$ weakens due to the stress-associated dissolution though the wear volume increases compared to that in dry case. Both the water-associated dissolution itself and induced delamination promote the sliding wear of CaF$_2$ in water. The results may help elucidate the water-associated wear mechanism of CaF$_2$ and optimize the processing parameters in the ultra-precision machining to reduce the residual surface/subsurface defects.

1. Introduction

Single crystal calcium fluoride (CaF$_2$) has been extensively used as one of the key materials of optical lens in extreme ultraviolet lithography due to its distinctive light transmission capacity and refractive index [1,2]. CaF$_2$ lens with ultra-precision surface quality, such as sub-nanometer surface roughness and minimum residual surface damage, is urgently required to promote its optical performance. To manufacture ultra-precision CaF$_2$ surface, developing the technique or method for achieving controllable material removal and reducing the residual surface damage is of crucial importance [3].

In the ultra-precision machining of CaF$_2$ crystal, the surface quality is found to be sensitive to the manufacturing environment [4]. A smooth CaF$_2$ surface without visible residual degradation can be fabricated in dry air; in contrast, massive surface defects are formed on the manufactured surface under water condition. These different surface characteristics are considered as the non-uniform distribution of stress beneath the working surface due to the rapid cooling by water. However, the water molecules between diamond tool and CaF$_2$ surface may

not only play role in the cooling or lubrication, but also participate in the tribological reactions during the machining process [5,6]. As an ionic crystal, CaF$_2$ is somewhat susceptible to water. In humid condition, water molecules can be adsorbed on the solid surface, and gradually grow up as water cluster or film with the increase of relative humidity (RH) [7–10]. A recent investigation using vibrational sum frequency generation spectroscopy detects that the ions dissolution in liquid water results in a CaF$_2$ surface with small positive charge [11]. Therefore, water, either vapor or liquid, may have a strong influence on the surface quality in the ultra-precision manufacturing process, but the corresponding removal mechanism of CaF$_2$ impacted by water has not been well addressed.

Previous studies have shown that water plays a significant role in surface wear or surface damage of some other brittle materials. For instance, single crystal silicon (Si) is easily worn out in humid air when sliding against silica micro-ball at an extremely low contact pressure, but the stress at that low level is insufficient to induce Si wear in dry or vacuum condition [12]. The increase of water vapor pressure can facilitate the material removal of Si [13]. Another example is the water-

---
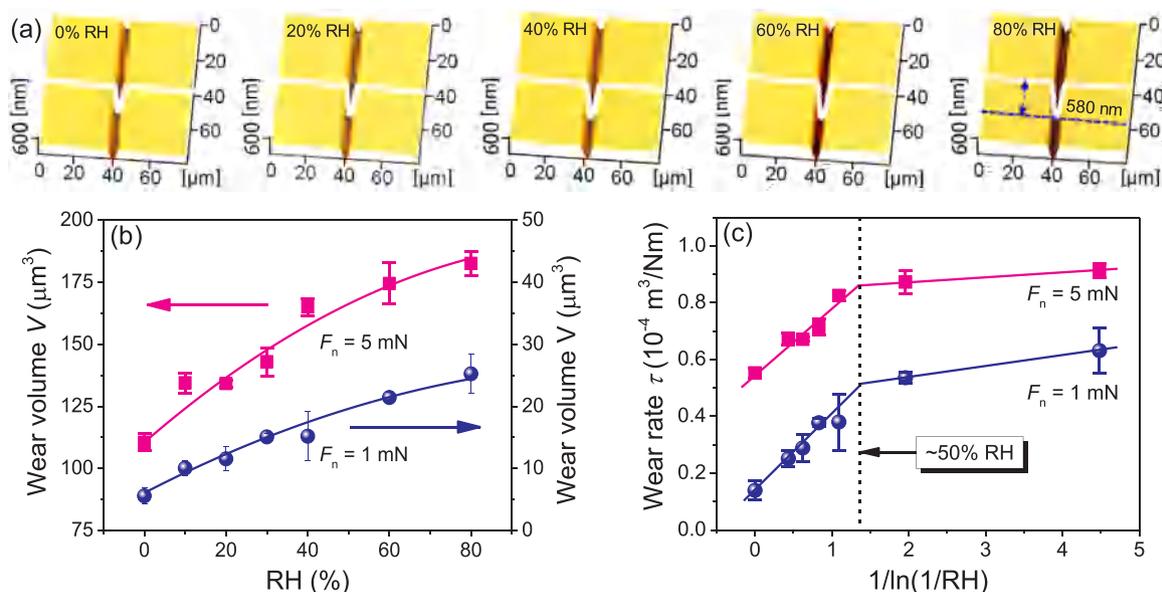
Fig. 1. CaF$_2$ wear as RH ranging from 0% to 80%. (a) AFM images and corresponding cross-section profiles of the wear scars formed after 25 sliding cycles at a normal load F_n of 5 mN. (b) Wear volume V as a function of RH. (c) Wear rate τ as a function of $1/\ln(1/RH)$. The lines are present as a guide to the eye. Wear rate is calculated from $\tau = V/(F_n L)$, where L is total sliding distance.
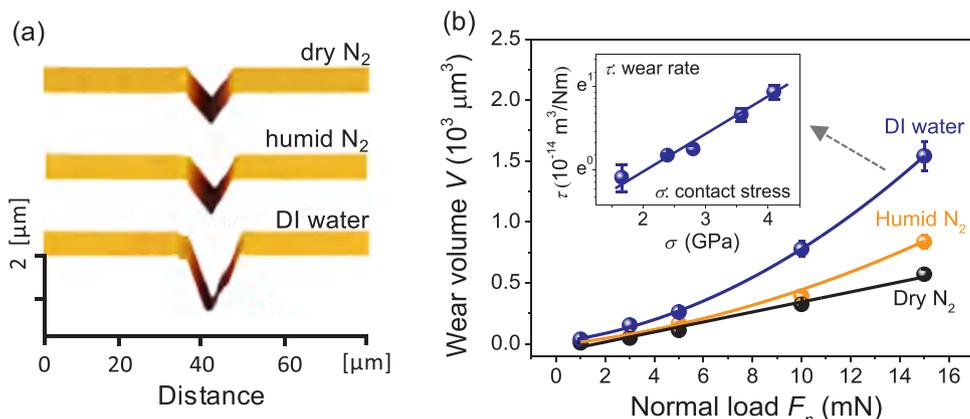
Fig. 2. Normal load dependence of CaF$_2$ wear in dry nitrogen, humid nitrogen (RH = 40 ± 2%) and DI water. (a) AFM images of the wear scars on CaF$_2$ surfaces obtained in the three environments under a representative load of 10 mN. (b) Wear volume V as a function of normal load F_n in the three environments. Inset: wear rate of CaF$_2$ as a function of average contact stress in DI water is fitted well by an exponential relationship. F_n increases from 1 mN to 15 mN. Sliding cycles are 25.

associated wear of glass under mechanical shear stress. Compared with the dry condition, the wear volume of glass increases in humid air or water, and the surface defects such as cracks easily formed under dry condition also are suppressed [14]. Contrary effect of water is found on the surface wear of potassium dihydrogen phosphate (KDP) crystal. Due to the ions dissolution, obvious surface defects (i.e., corrosion pits) are formed on the KDP surface when the surface material is removed in humid air or in water solution, but there is almost no defects when water is eliminated in the working environment [15]. Generally, the diverse surface characteristics observed in dry and water conditions suggest that different wear mechanisms impacted by water may be responsible for the material removal process.

In this study, sliding experiments of CaF$_2$(111) against a diamond tip were performed in dry nitrogen, humid conditions with various RH and deionized (DI) water to detect the role of water in the material removal of CaF$_2$. With the increase of RH, the wear of CaF$_2$ was found to increase with a linear relationship between wear rate and $1/\ln(1/RH)$. Furthermore, significantly different applied load dependence of wear behaviors were observed in dry nitrogen and in moisture conditions, indicating change of the wear mechanism involved in the wear process. The corresponding mechanisms were discussed based on the dominated contribution of stress-induced plastic flow in dry condition, or stress-enhanced dissolution and delamination in different water-

containing environments.

2. Experimental methods

The samples are polished CaF$_2$(111) wafers. By using atomic force microscopy (AFM, SPI3800N, Seiko, Japan), root-mean-square (RMS) roughness of the CaF$_2$ surface was measured as around 0.12 nm over a 1 μm^2 area by a sharp Si$_3$N$_4$ tip (MLCT, Veeco, USA) with a curvature radius less than 20 nm. Before the experiments, the CaF$_2$ wafers were ultrasonically cleaned in ethanol for ∼ 3 min to remove possible adsorbed contaminates, following washed by DI water and dried in pure nitrogen.

The wear tests of CaF$_2$ surface slid against a conical diamond tip (radius = ∼ 25 μm) were performed with reciprocating method using an environmentally controllable scratch instrument connected an external vapor control system. The sliding direction was along [11−2] (or [-1−12]) orientation. To detect the role of water in CaF$_2$ wear, material removal in three environments, including dry nitrogen, humid nitrogen (RH = 40 ± 2%) and DI water were studied. The dry and humid environments were realized by a vapor control system controlling the flow rate of nitrogen through DI water. More details of this method have been described in previous literature [16]. The pH of the DI water is 5.7 ± 0.2. All the experiments were performed under room
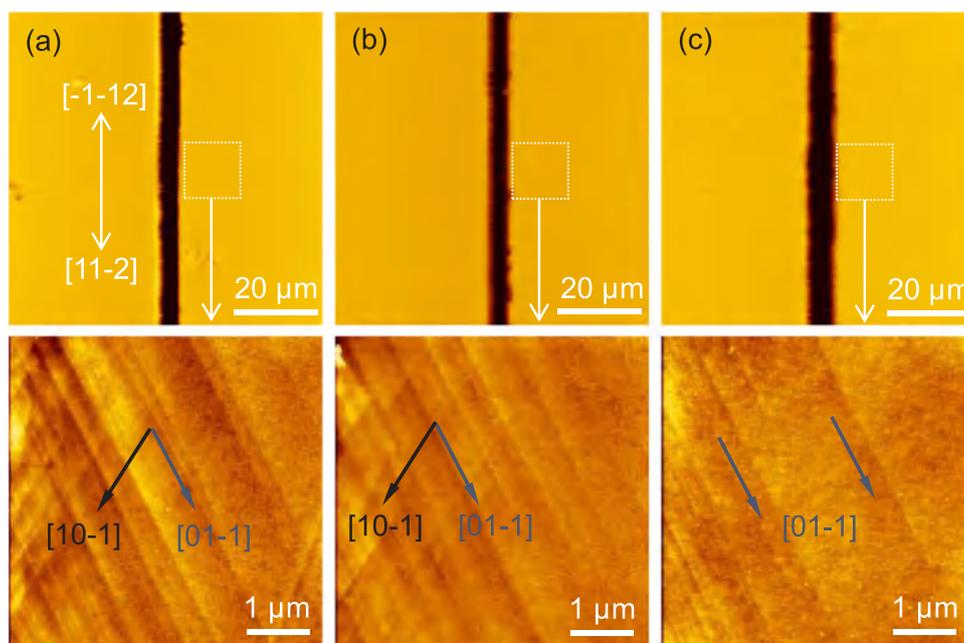
Fig. 3. AFM images showing the occurrence of slip in dry nitrogen (a), humid nitrogen (b) and DI water (c) under a normal load of 5 mN.

temperature, and the applied normal load F_n ranged from 1 mN to 15 mN, the sliding speed v was 100 μm/s, the number of sliding cycle was 25. Each sliding wear test was repeated 3 times at least. After the sliding wear tests, topographies of the wear scars were obtained using AFM with the sharp Si_3N_4 tips. The worn surfaces were characterized by scanning electron microscopy (SEM, Quanta FEG 250, FEI, USA). The contents and chemical bonds of the worn surfaces formed in the different environments were analyzed by X-ray photoelectron spectra (XPS, XSAM800, Kratos, UK). The chemical compositions of CaF_2 surfaces before and after immersed in DI water were analyzed by Raman spectroscopy (InVia, Renishaw, England).

3. Results and discussion

3.1. Humidity dependence of CaF_2 wear

Material removal of CaF_2 slid against a diamond tip was studied as RH increasing from 0% to 80%. Fig. 1a shows the topographies and corresponding cross-section profiles of the wear scars formed at a representative normal load of 5 mN in various RH conditions. CaF_2 wear increases substantially as RH goes up. After 25 sliding cycles, wear depth of the formed wear scar is ~ 420 nm in dry nitrogen, and increases to ~ 580 nm in 80% RH nitrogen. The load dependence of wear volumes V estimated at the normal loads of 1 mN and 5 mN are plotted in Fig. 1b. The wear volumes increase sharply in low RH range, and slowly in high RH range. When the wear rate τ is plotted against $1/\ln(1/RH)$, linear dependence is displayed in the entire RH range; however, there is a critical RH around 50% above which the slops of τ - $1/\ln(1/RH)$ curve decrease both at the normal loads of 1 mN and 5 mN (Fig. 1c).

The results in Fig. 1 indicates that water in humid nitrogen has a significant role in facilitating CaF_2 wear. Physically, water can condense around the sliding contact and form a meniscus around the annulus of the contact area because of the capillary effect [17,18]. As the growth of the meniscus is considered as a thermally activated process, RH dependence of the meniscus volume V_m is found to be proportional to $1/\ln(1/RH)$ [19], which is similar to the dependence of CaF_2 wear (Fig. 1c). In other words, there is a linear relationship between the wear rate τ and the amount of adsorbed water involved in the water meniscus.

$$\tau \propto 1/\ln(1/RH) \propto V_m \tag{1}$$

However, the different slops of τ - $1/\ln(1/RH)$ curves in the low and high RHs (Fig. 1c) indicate that the role of water molecules involved in CaF_2 wear may change. A similar transition from the strongly linear $[1/\ln(1/RH)]$ dependence of wear rate to the weak dependence was reported for the wear of the hydroxyl terminated silicon [12]. One commonality between Si and CaF_2 surfaces is their capability to adsorb water molecules from humid air [20]. In low RH, the water adsorbed on the silicon surface is dominated by strongly hydrogen bonded network, which have higher contribution to the silicon wear than the weakly hydrogen-bonded water growing in high RH [21]. Then, we hypothesize that the change of the slops of τ - $1/\ln(1/RH)$ curves (Fig. 2c) may correspond to the diverse mechanism or dynamics through which water molecules are involved in the CaF_2 wear. However, more details into molecular configuration of the adsorbed water on CaF_2 surface may require characterization, which are the subject of a future work.

3.2. Load dependence of wear behaviors in the different environments

CaF_2 wear can be facilitated by water that strongly depends on the water amount (Fig. 1). To detect the role of water in CaF_2 wear, material removal were studied in dry nitrogen, humid nitrogen and DI water respectively as the normal load increased from 1 mN to 15 mN. Fig. 2a shows representative topographies of the wear scars on CaF_2 surfaces formed in these three environments under an applied load of 10 mN. When the sliding wear test is operated in dry nitrogen (RH = 0%), a wear scar with a depth of ~790 nm is formed on CaF_2 surface after 25 sliding cycles. Under the same experimental conditions, the wear depth reaches to ~ 920 nm in humid nitrogen, and further increases to ~ 1400 nm in DI water. The results demonstrate that the water molecules from adsorption layer or liquid solution can facilitate the wear of CaF_2 surface when slid against the diamond tip.

The wear volume as a function of normal load plotted in Fig. 2b suggests that the wear behaviors in the three environments cannot be described by a single wear relationship. Here, a strong linear relationship between wear volume V and normal force F_n is observed only in dry condition, which follows the Archard wear equation developed based on the fully plastic removal of material, as below [22],
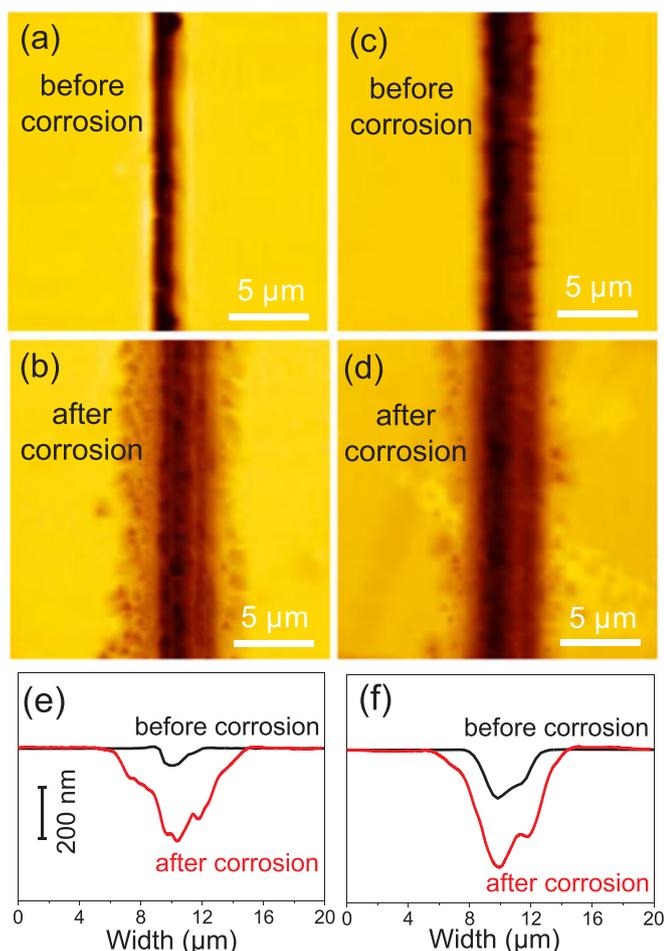
Fig. 4. Comparison of the etched wear tracks formed in dry nitrogen and DI water. a and b respectively show the wear track formed in dry nitrogen before and after etching in 50 wt% sulfuric acid solution. c and d respectively show wear track formed in DI water before and after etching treatment. e and f compare cross-section profiles of the wear tracks formed under these two environments. The applied load in sliding tests is 1 mN. The corrosion time during etching treatment is ~ 5 min, and the solution temperature keeps at ~ 60 °C.

$$V = k\frac{F_n L}{H}, \qquad (2)$$

where the sliding distance L is 80 μm, the hardness H of CaF$_2$ is ~ 2.5 GPa. Then, the wear coefficient k in Eq. (2) implies that the degree of the mechanical wear can be estimated at ~ 0.70.

Under the same normal load, the wear volume is the smallest in dry nitrogen, and the largest in DI water. Fig. 2b shows that Archard wear equation fails to capture the wear behaviors of CaF$_2$ in water-containing environments. To quantitatively describe the wear behavior of CaF$_2$ in DI water, wear rate τ is plotted as a function of average contact stress σ estimated by Hertz contact model ($\sigma = F_n/A$, A is the Hertz contact area), as shown in the inset of Fig. 2b. Analysis shows that an exponential dependence of wear rate on average contact stress can fit the data especially obtained in DI water, which can not be described using Archard wear equation.

The different load dependent wear behaviors of CaF$_2$ in dry nitrogen and water-containing environments imply that the wear mechanism changes as water molecules participate in the CaF$_2$ wear process. No visible changes of the diamond tips before and after the wear tests in the three environments are observed by high resolution light microscopy, indicating that the impact of tip wear on the different CaF$_2$ wear behaviors can be ruled out. Due to the absence of water in dry condition, material removal on CaF$_2$ surface slid against the inert diamond

tip is dominated by mechanical interaction [23]. Although mechanical wear normally corresponds to plastic deformation, viscous flow of materials or/and fracture [24,25], the load dependence of wear volume predicted well by Archard wear equation (Fig. 2b) suggests that plastic wear may dominate the material removal of CaF$_2$ in dry condition. When the sliding tests are conducted in water-containing environments, the increased wear volume indicates that the water-associated reactions should contribute to material removal of CaF$_2$. However, the degree of reactions between CaF$_2$ surface and water molecules under shear stress strongly depends on the amount of water. It is noteworthy that the reaction between CaF$_2$ and water caused by mechanical stress may be different from the tribochemical reactions reported previously. Take an example of Si, tribochemical wear occurs with the necessary bonding bridge formed at the tribological interface [21,26,27]. Due to the high chemical inertness, the diamond tip can hardly form chemical bonding bridge between the sliding interface so that the tribochemical reaction is absent on Si surface both in dry and humid conditions [28]. Here, water-associated reaction occurs on CaF$_2$ surface although the interfacial bonding bridge is difficult to form at the CaF$_2$/diamond interface.

3.3. Change of worn surface and wear debris characteristics caused by water

CaF$_2$ is a face-centered cubic crystal and its primary slip system is {100} plane with < 110 > direction, so the plastic flow or plastic deformation occurring in the sliding process strongly relates to the slip system [29]. The sliding directions in this study is [11 − 2] or [-1 − 12]. As shown in Fig. 3, slip lines appear with angles of ± 30° to the sliding direction on both sides of the wear track, indicating that the slip systems of [10 − 1] and [01 − 1] (or [-101] and [0 − 11]) on {100} surface are activated [30]. In dry nitrogen, the slip of CaF$_2$ (Fig. 3a) suppresses the generation of fracture and causes uniform plastic flow of CaF$_2$ material, which can explain the formation of the smooth worn surface shown in Fig. 4a. Compared to the wear track produced in dry nitrogen, less slip lines around the wear tracks are observed in humid nitrogen and DI water (Fig. 3b and c), implying that the contribution of plastic wear to CaF$_2$ wear decreases when water molecules participate into the material removal process.

The activation of slip system generates plastic deformation due to dislocation movement, therefore, the extent of plastic deformation can also be revealed by dislocation site density. Site-selective etching at plastic deformation region by acid etchant such as phosphoric acid and sulfuric acid is an appropriate way to reveal the dislocation site, which can generate corrosion pits after etching treatment [31]. Therefore, the difference of plastic wear formed in various environments was deeply characterized through etched in 50 wt% sulfuric acid solution. Before etching, wear tracks with a depth of ~ 80 nm and ~ 200 nm were respectively formed in dry nitrogen and DI water at a normal load of 1 mN (Fig. 4a and c). After the corrosion treatments, the surface damage in these two conditions become similar (Fig. 4b and d). It means that much more CaF$_2$ material is etched for the wear track formed in dry nitrogen compared to that in DI water (Fig. 4e and f). Furthermore, more corrosion pits appearing around the wear track formed in dry nitrogen than that in DI water. The results support that water can significantly weaken the plastic wear of CaF$_2$ crystal.

Topographies in worn regions were imaged by SEM to further detect the influence of water on CaF$_2$ wear. The SEM image of worn region formed in dry nitrogen shows a relatively smooth worn surface (Fig. 5a and d), ruling out the occurrence of fracture in the CaF$_2$ wear under the given load conditions. The result confirms that the material removal on CaF$_2$ surface in dry condition is mainly attributed to the stress-driven plastic wear [29]. Compared to the case in dry nitrogen, a relatively smooth surface is formed in humid environment besides the generation of obvious micro-pits in part worn regions (Fig. 5b and e), which gives a strong evidence that CaF$_2$ is removed via water-associated reaction to some extent in addition to plastic wear. The topography of worn surface
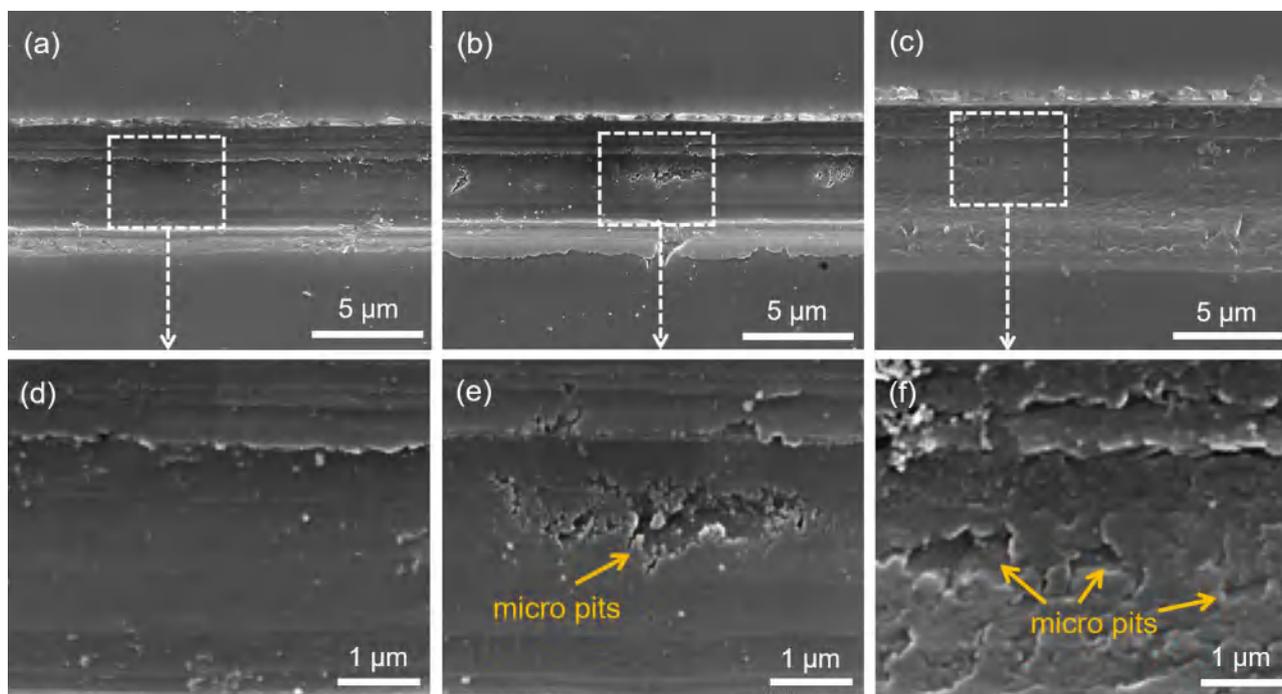
Fig. 5. SEM images of the wear scars formed in dry nitrogen (a), humid nitrogen with RH of 40 ± 2% (b) and DI water (c) under a normal load of 5 mN. d-f show the details of the corresponding worn regions marked in a-c, respectively.
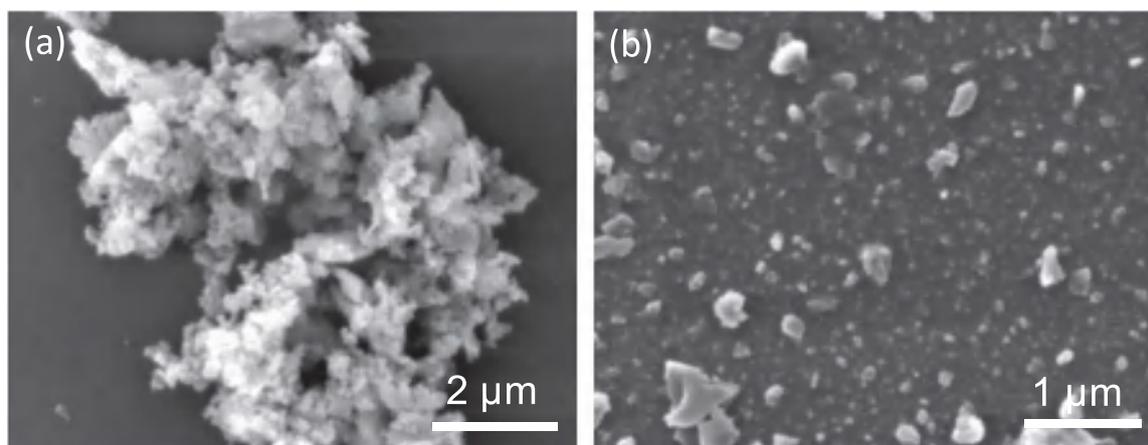
Fig. 6. SEM images of the wear debris formed in dry nitrogen (a) and DI water (b) under a normal load of 5 mN.

formed in DI water is greatly different from the case in dry nitrogen. SEM images in Fig. 5c and f show a much rougher surface with lots of micro pits inside the wear track formed in DI water.

Previous studies reported the contrary wear behaviors of other materials affected by water, such as SiC, Si_3N_4 and glass [14,32,33]. In dry condition, material removal dominated by mechanical interaction causes a rough worn surface due to the occurrence of fracture. Whereas in water-containing condition, the fact that chemical reaction with water under mechanical stress inducing atomic attrition or formed reaction products lubricating the sliding interface results in a relatively smooth worn- surface. Different from the mentioned main-covalent materials, the CaF_2 as an ionic crystal can dissolve in water due to the degradation of electrostatic force between Ca^{2+} and F^- ions [34]. During the sliding process, compressive or shear stress can lower the energy barrier for ionic bonds breaking, and then accelerate the dissolution of surface ions. This process is commonly depicted as the stress-enhanced dissolution [35].

Given the less plastic damage (Fig. 4) and the distinctive surface topographies (Fig. 5c) formed in DI water, we therefore presume that

CaF_2 wear in DI water may originates from water-associated dissolution under the mechanical stress. On the one hand, water-associated dissolution itself can facilitate the CaF_2 wear. On the other hand, dissolution may promote initiation and propagation of crack under shear or tensile stress and finally cause material spalling [34]. Fig. 6a and b respectively show wear debris formed in dry nitrogen and DI water. The formation of flake in DI water (Fig. 6b) but is absent in dry nitrogen (Fig. 6a) supports the occurrence of material spalling under water conditions. The similar phenomenon has been reported in single point diamond cutting of KDP. Water-associated ions dissolution is found to play a significant role in the material removal of KDP surface, resulting in the formation of rougher fabricated surface with more defects at higher RHs [15].

3.4. Dissolution wear of CaF_2 characterized by XPS and Raman measurements

Ex situ XPS analysis was conducted to find the possible change of surface chemical compositions in the worn region and the wear debris
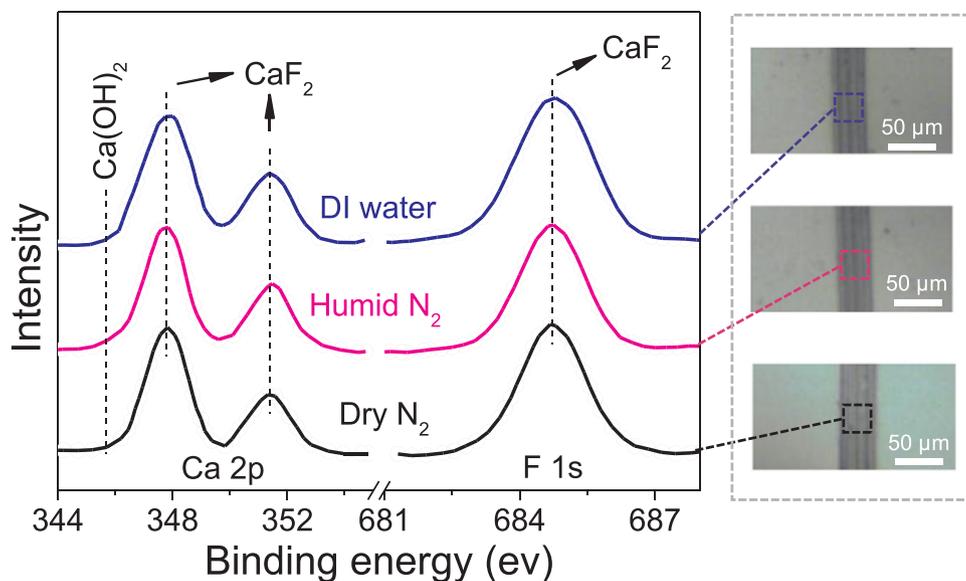
Fig. 7. Ca 2p and F 1s X-ray spectra in worn regions formed in dry nitrogen, humid nitrogen (RH = 40%) and DI water. Right insets show the wear tracks formed in three conditions which were used for XPS measurements.
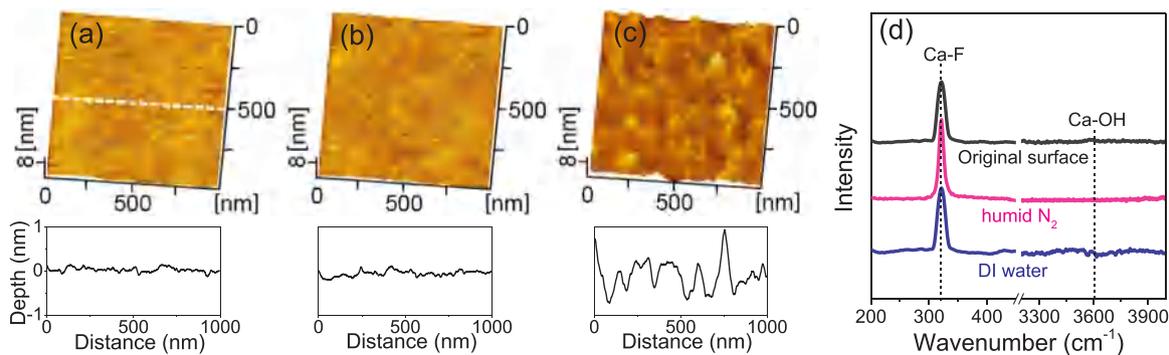
Fig. 8. AFM images of CaF$_2$ surfaces before (a) and after exposed 4 h in humid nitrogen (b) and DI water (c). (d) shows the Raman spectra measured on the three surfaces.
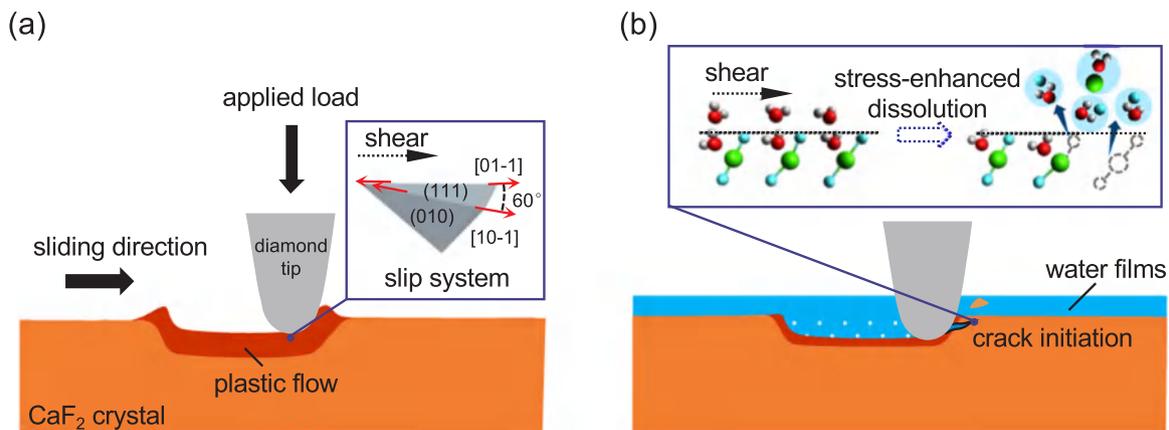
Fig. 9. The schematics showing sliding wear of CaF$_2$ against diamond tip dominated by plastic wear in dry nitrogen (a) and by stress-enhanced dissolution in DI water (b). Upper-right picture in (a) shows the activation of the slip systems on {100} plane with [10−1] and [01−1] (or [-101] and [0−11]) directions. Upper inset in (b) shows the stress-enhanced ions dissolution process of CaF$_2$ in DI water, which may promote the crack initiation and cause material spalling. The atoms of calcium and fluorine in CaF$_2$, oxygen and hydrogen in water molecule are marked by cyan, light blue, red and gray colors, respectively. The possible plastic deformation regions between diamond tip and CaF$_2$ substrate marked by deep red color are schematically compared in dry condition and in DI water.

formed in the different environments. Before XPS measurements, the CaF$_2$ samples with larger wear scars (width > 40 μm) are prepared under a normal load of 5 mN using scanning model (right insets in Fig. 7). Fig. 7 compares Ca 2p and F 1s XPS spectra taken from the worn regions formed in dry nitrogen, humid nitrogen and DI water. Similar XPS spectra of Ca 2p and F 1s are obtained in the measurements of the wear debris formed in the three environments, so the results are not shown here. The Ca 2p peaks at 347.6 eV and 351.5 eV, and the F 1s peak at 685.1 eV are assigned to be CaF$_2$ [36]. In all cases, the Ca 2p and F 1s peak shapes are very similar to each other, and no shift of each peak is observed, regardless of the sliding test environments. Based on the data shown in Fig. 7 and the corrected relative sensitivity factors, the atomic ratios of F/Ca are estimated at around 1.5 in all the given atmospheres. Furthermore, no visible Ca 2p peaks at 345.5 eV, corresponding to Ca(OH)$_2$ [37], are observed in all worn regions, indicating that the chemical reaction product is below the detection limit both in dry and water conditions. Furthermore, since the DI water used in this study is weakly acid (pH = 5.7 ± 0.2), Ca^{2+} and F$^-$ ions may dissolve directly [11]. Then, tribochemical reaction, such as CaF$_2$ crystal reacting with water to form calcium hydroxide, may be very limited during the sliding process.

The evolution of surface topographies in humid nitrogen (RH = 40%) and DI water was characterized by AFM to check the occurrence of ions dissolution induced by water. Fig. 8a shows the AFM image and corresponding section profile of the original CaF$_2$ surface. The surface roughness is around 0.12 nm over an area of 1 μm^2. After exposed 4 h in humid nitrogen, no apparent change in topography is observed on the CaF$_2$ surface, as shown in Fig. 8b. However, obvious corrosion pits appear on the CaF$_2$ surface after immersed 4 h in DI water, and the RMS roughness increases to 0.67 nm (Fig. 8c). Fig. 8d demonstrates the Raman spectra measured on the three surfaces. The peaks at ~ 320 cm^{-1} are ascribed to be Ca-F bonds [38]. It is worth to notice that the intensity of peak at ~ 3600 cm^{-1} corresponding to calcium hydroxide is below the limit of detection [39], consistent with the results obtained in XPS analysis (Fig. 7). Actually, the ionic bonds between Ca^{2+} and F$^-$ ions are relatively strong, and the ionic dissolution depends on several factors, such as the ions concentration in water, dissolution time and temperature [40,41]. The results indicate that ions dissolution of CaF$_2$ that occurs in the weakly acid DI water (Fig. 8c) can be facilitated by the mechanical shear stress during sliding process (Figs. 1 and 2).

3.5. Wear mechanisms of CaF$_2$ crystal in dry and water-containing conditions

Fig. 9 schematically shows the removal processes of CaF$_2$ slid against a diamond tip in dry nitrogen and DI water. In dry condition, plastic wear dominates the material removal of CaF$_2$ under the given load conditions, as shown in Fig. 9a. The activation of the slip systems on {100} plane with [10−1] and [01−1] (or [-101] and [0−11]) directions (upper-right picture in Fig. 9a) results in a relatively smooth worn-surface (Fig. 5a). When the sliding tests are operated in water-containing environments, stress-enhanced dissolution has a significant contribution to the CaF$_2$ wear. The critical process for CaF$_2$ wear caused by water-associated dissolution can be conceived as three stages (Fig. 9b) (i) stretching of Ca-F bonds by mechanical shear stress which lowers the activation energy barrier for bonds rupture, (ii) associative or physical adsorption of water molecules at CaF$_2$ surface via van der Waals force [8], and (iii) degradation of the Coulombic attractions between Ca^{2+} and F$^-$ ions by adsorbed water molecules via dipole interactions, assisting the stretched bonds rupture [42], and then leading to the dissolution of Ca^{2+} and F$^-$ ions in water. Moreover, dissolution may promote crack initiation under mechanical stress and finally cause material delamination.

Generally, water was found to facilitate the CaF$_2$ wear, but be capable of reducing the plastic damage. Normally, activation of slip

systems in different directions results in anisotropic wear of CaF$_2$ material, resulting in the decrease of machined surface quality [23,43,44]. This study provides a new insight into the process optimization for ultra-precision surface manufacturing that enhancement of the dissolution can suppress the inconsistent removal of CaF$_2$ material to some extent. However, further research is needed to balance the negative contribution to the increase of manufactured surface roughness.

4. Conclusion

In the present work, the influence of water on material removal of CaF$_2$ (111) was studied upon a scratch tester with a conical diamond tip. With the increase of RH, the wear of CaF$_2$ was found to increase with a linear relationship between τ and $1/[\ln(1/RH)]$. There is a strong relationship between normal load (contact stress) and wear volume (wear rate), which cannot be described by single wear model in different environments. The wear behavior follows the Archard wear equation in dry nitrogen, but shows an exponential dependence in DI water. Due to the activation of slip system under mechanical shear stress, the domination of plastic flow in dry condition results in a relatively smooth worn surface. Differently, plastic damage of CaF$_2$ material is suppressed to some extent, and water-associated dissolution and material delamination play a significant role in CaF$_2$ wear under water-containing conditions.

References

[1] C. Wagner, N. Harned, EUV lithography: lithography gets extreme, Nat. Photonics 4 (2011) 24–26.

[2] J. Sils, S. Hausfeld, W. Clauß, U. Pahl, R. Lindner, M. Reichling, Impurities in synthetic fluorite for deep ultraviolet optical applications, J. Appl. Phys. 106 (2009) 063109.

[3] R.S. Retherford, R. Sabia, V.P. Sokira, Effect of surface quality on transmission performance for (111) CaF$_2$, Appl. Surf. Sci. 183 (3–4) (2001) 264–269.

[4] J. Yan, J. Tamaki, K. Syoji, T. Kuriyagawa, Single-point diamond turning of CaF$_2$ for nanometric surface, Int. J. Adv. Manuf. Technol. 24 (2004) 640–646.

[5] K.A. Becraft, G.L. Richmond, In situ vibrational spectroscopic studies of the CaF$_2$/H$_2$O interface, Langmuir 17 (2001) 7721–7724.

[6] N. Kobayashi, S. Itakura, H. Asakawa, T. Fukuma, Atomic-scale processes at the fluorite−water interface visualized by frequency modulation atomic force microscopy, J. Phys. Chem. 117 (2013) 24388–24396.

[7] M. Cardellach, A. Verdaguer, J. Fraxedas, Defect-induced wetting on BaF$_2$(111) and CaF$_2$(111) at ambient conditions, Surf. Sci. 605 (2011) 1929–1933.

[8] N.H. de Leeuw, T.G. Cooper, A computational study of the surface structure and reactivity of calcium fluoride, J. Mater. Chem. 13 (2003) 93–101.

[9] K. Miura, T. Yamada, M. Ishikawa, S. Okita, Apparent contrast of molecularly thin films of water at ionic crystal surfaces, Appl. Surf. Sci. 140 (1999) 415–421.

[10] L. Chen, C. Xiao, B.J. Yu, S.H. Kim, L.M. Qian, What governs friction of silicon oxide in humid environment: contact area between solids, water meniscus around the contact, or water layer structure, Langmuir 33 (2017) 9673–9679.

[11] R. Khatib, H. Ellen, G. Backus, M. Perez-Haro, M. Gaigeot, M. Sulpizi, Water orientation and hydrogen bond structure at the fluorite/water interface, Sci. Rep. 6 (2016) 24287.

[12] L. Chen, H.T. He, X.D. Wang, S.H. Kim, L.M. Qian, Tribology of Si/SiO$_2$ in humid air: transition from severe chemical wear to wearless behavior at nanoscale, Langmuir 31 (2015) 149–156.

[13] C. Chen, C. Xiao, X.D. Wang, P. Zhang, L. Chen, L.M. Qian, Role of water in the tribochemical removal of bare silicon, Appl. Surf. Sci. 390 (2016) 696–702.

[14] H.T. He, L.M. Qian, C.G. Pantano, S.H. Kim, Mechanochemical wear of soda lime silica glass in humid environments, J. Am. Ceram. Soc. 97 (7) (2014) 2061–2068.

[15] M.R. Kozlowski, I. Thomas, G.K. Edwards Stanion, K. Stanion, B. Fuchs, Influence of diamond turning and surface cleaning processes on the degradation of KDP crystal surfaces, Proc. Spie 1561 (1991) 59–69.

[16] C. Xiao, J. Guo, P. Zhang, L. Chen, L.M. Qian, Effect of crystal plane orientation on tribochemical removal of monocrystalline silicon, Sci. Rep. 7 (2017) 40750.

[17] L. Bocquet, E. Charlaix, S. Ciliberto, J. Crassous, Moisture-induced ageing in granular media and the kinetics of capillary condensation, Nature 396 (6713) (1998) 735–737.

[18] O. Noel, P.E. Mazeran, H. Nasrallah, Sliding velocity dependence of adhesion in a nanometer-sized contact, Phys. Rev. Lett. 108 (2012) 015503.

[19] E. Riedo, F. Lévy, H. Brune, Kinetics of capillary condensation in nanoscopic sliding friction, Phys. Rev. Lett. 88 (18) (2012) 185505.

[20] L. Chen, X. He, H.S. Liu, L.M. Qian, S.H. Kim, Water adsorption on hydrophilic and hydrophobic surface of silicon, J. Phys. Chem. C 122 (2018) 11385–11391.

[21] X.D. Wang, S.H. Kim, C. Chen, L. Chen, H.T. He, L.M. Qian, Humidity dependence of tribochemical wear of monocrystalline silicon, ACS Appl. Mater. Interfaces 7 (2015) 14785–14792.

[22] J.F. Archard, Wear theory and mechanisms, in: M.B. Peterson, W.O. Winer (Eds.), Wear Control Handbook, ASME, New York, 1980, pp. 35–80.

[23] L. Chen, L.C. Hu, C. Xiao, Y.Q. Qi, B.J. Yu, L.M. Qian, Effect of crystallographic orientation on mechanical removal of CaF_2, Wear 376–377 (2017) 409–416.

[24] R. Khanna, B. Basu, Sliding wear properties of self-mated yttria-stabilized tetragonal zirconia ceramics in cryogenic environment, J. Am. Ceram. Soc. 90 (8) (2007) 2525–2534.

[25] G.W. Stachowiak, Wear-Materials, Mechanisms and Practice, J Wiley, West Sussex, 2006.

[26] L. Chen, C. Xiao, X. He, B.J. Yu, S.H. Kim, L.M. Qian, Friction and tribochemical wear behaviors of native oxide layer on silicon at nanoscale, Tribol. Lett. 65 (2017) 139.

[27] L. Chen, J.L. Wen, P. Zhang, B.J. Yu, C. Chen, T.B. Ma, X.C. Lu, S.H. Kim, L.M. Qian, Nanomanufacturing of silicon surface with a single atomic layer precision via mechanochemical reactions, Nat. Commun. 9 (2018) 1542.

[28] C. Xiao, C. Chen, J. Guo, P. Zhang, L. Chen, L.M. Qian, Threshold contact pressure for the material removal on monocrystalline silicon by SiO_2 microsphere, Wear 376 (2017) 188–193.

[29] S. Azamia, H. Kudo, Y. Mizumoto, T. Tanabe, J. Yan, Y. Kakinuma, Experimental study of crystal anisotropy based on ultra-precision cylindrical turning of single-crystal calcium fluoride, Precis. Eng. 40 (2015) 172–181.

[30] K. Niki, G. Mochimaru, H. Shindo, Participation of {100} < 011 > slip system in sliding friction at (001), (111) and (110) surface of fluorite (CaF_2) crystal, Tribol. Online 7 (2017) 81–86.

[31] C. Motzer, M. Reichling, High resolution study of etch figures on $CaF_2(111)$, J. Appl. Phys. 105 (2009) 064309.

[32] K.H. Zum Gahr, R. Blattner, D.H. Hwang, K. Pöhlmann, Micro- and macro-tribological properties of SiC ceramics in sliding contact, Wear 250 (2001) 299–310.

[33] S. Sasaki, The effects of the surrounding atmosphere on the friction and wear of alumina, zirconia, silicon carbide and silicon nitride, Wear 134 (1989) 185–200.

[34] T.A. Michalske, B.C. Bunker, Stress corrosion of ionic and mixed ionic/covalent solids, J. Am. Ceram. Soc. 69 (1986) 721–724.

[35] J.T. Dickinson, N.S. Park, M.W. Kim, S.C. Langford, A scanning force microscope study of a tribochemical system: stress-enhanced dissolution, Tribol. Lett. 3 (1997) 69–80.

[36] Y.T. Wu, J.T. Mayer, E. Garfunkel, T.E. Madey, X-ray photoelectron spectroscopy study of water adsorption on $BaF_2(111)$ and $CaF_2(111)$ surfaces, Langmuir 10 (1994) 1482–1487.

[37] H.U.V. Gertha, T. Dammaschke, E. Schafer, H. Züchner, A three layer structure model of fluoridated enamel containing CaF_2, $Ca(OH)_2$ and FAp, Dent. Mater. 23 (2007) 1521–1528.

[38] H. Tsuda, J. Arends, Detection and quantification of calcium fluoride using micro-raman spectroscopy, Caries Res. 27 (1993) 249–257.

[39] T. Schmid, P. Dariz, Shedding light onto the spectra of lime: raman and luminescence bands of CaO, $Ca(OH)_2$ and $CaCO_3$, J. Raman Spectrosc. 46 (1) (2014) 141–146.

[40] C. Erickson, Nanoscale Wear on the Fluorite (CaF_2) [111] Cleavage Plane, Masteral Dissertation, Washington State University, 2013.

[41] G. Jordan, W. Rammensee, Growth and dissolution on the CaF_2 (111) surface observed by scanning force microscopy, Surf. Sci. 371 (1997) 371–380.

[42] J.N. Israelachvili, Intermolecular and Surface Forces, Elsevier INC press, NY, 2012.

[43] Y. Mizumoto, Y. Kakinuma, Revisit of the anisotropic deformation behavior of single-crystal CaF_2 in orthogonal cutting, Precis. Eng. (2018), https://doi.org/10.1016/j.precisioneng.2018.01.011.

[44] Y. Mizumoto, T. Aoyama, Y. Kakinuma, Basic study on ultraprecision machining of single-crystal calcium fluoride, Procedia Eng. 19 (2011) 264–269.